

An Implementation of Cardiovascular Disease Prediction in Ultrasonography Images using AWMYOLOv4 Deep Learning Mode

***¹Damodharan D and ²Amit Kumar Goel**

^{*1}Computer Science and Engineering, Research scholar & Assistant Professor, Galgotias University, Greater Noida, 201308, India

²Computer Science and Engineering, Professor, Galgotias University, Greater Noida, 201308, India

^{*1} rpaper732@gmail.com , ² amit.goel@galgotiasuniversity.edu.in

***Corresponding Author:** Damodharan D, rpaper732@gmail.com

Abstract:

Cardiovascular diseases are one of the most important issues facing the people and their origins also death is contained all over the world the facing issues in past 25 years. Every country's investing large amount in health care researches and it's related to enhanced predict the diseases. Cardio issues are not even physicians can easily be predicted and it is a very challenging task that requires high knowledge and expertise. To identify to create machine language models used to efficiently predict the earliest stage of cardiovascular disease. In this work, we recommend AWMF filter for the pre-process the Input Image after the input move to YOLOv4 neural network method for classification and segmentation to the heart affected areas by using ultrasonic Images with the help of a machine learning algorithm. The proposed algorithm uses ultrasonic picture classification and segmentation to detect cardiovascular disease earlier. This model shows the more accurate result on 96% of training and 98% testing data. And this method shows better results and providing while compared to the existing method.

Keywords: Adaptive weighted median filter, classification, cardiovascular diseases, Machine Learning, segmentation, ultrasonic image, YOLOv4.

1. Introduction

Nowadays people are not given more importance to their health due to workload, stress, food habit and lifestyle. And Every country's economically inverse large amount for health care researches and it's related to enhanced predict the diseases. To identify and create machine language models used to efficiently predict the earliest stage of cardiovascular disease. In the WHO survey in the global death rate, 17.9 million people are expired every year. The risk of disease is increased day by day. In China every year 30% of death are going to held by heart diseases[H] it is estimated that 290 million people are suffered from any one of heart issues and the death rate is also more than 40%. And Various factors are increasing diseases like uncontrolled food habits, large stressful work, hypertension, improper cholesterol level, etc... And Earlier diagnosis is the only solution for this problem, even though some misclassification of symptoms due to natural hazards they are not able to know about the CVD diseases sign and symptoms of this disease.

Various type of technologies is involved into the health care field for the analysis and diagnosis form the medical issues,

validating & verifying proper data. Especially in Medical technique's the machine learning is give more support to the health care system.[1]For examining the patient to identify the problem in her health and to eliminate the effect of instruments and operators, standardization of images is necessary. The stage of Pre-processing is select the raw images is necessary to eliminate noise, pieces and cardio tissues devoted to Ultrasound images. An individual may undergo a CT and MRI scan for diagnosis.

Upon comprehensively reviewing the current high-tech approaches, we found the various models to summarized in Table 1, that is Art and state for Critical analysis and comparison of study various characteristics, model/algorithm and the result.[2,3] As a result of noise reduction and muscle removal methods not being included in most classification techniques, a high rate of false positives and misclassifications occurs. A variety of techniques is available for classifying cardio images and extracting different features. Classifying heart diseases using deep learning frameworks is possible with a few techniques. Although high-resolution images can be involving to improve diagnosis, some factors may interfere, such as

instrument settings and heart values, as well as positioning by the operator.

Ultrasound (US) is one of the most useful imaging modalities in the medical field it has been recognized as the powerful screening and diagnosis tool for radiologists and physicians. US image is used works wide due to soft, safe without radiation and low cost. It has advantages over other medical imaging modalities such as X-Ray, MRI, CT, and non-ionizing radiations. [4] In addition, A second challenge facing US physicians is low imaging quality, noise contamination, and artifacts, as well as a high reliance on the hands-on experience of their surgeon. In order to achieve more accuracy, objective, and intelligent outcomes, US imaging analysis methods, as used in diagnosis and assessment, and image-guided interventions, are utilized. with deep learning, you can learn from and test images straight from the training data, which is why it is a subset of Machine learning.[5] The objective is to automatically discover a model that employs US image analysis techniques such as organ classification, segmentation, object recognition, and quality evaluation.

Similarly, segmentation is a critical component in both the medical and non-medical fields of image processing and analysis. Image segmentation involves the process of clustering pixels in a picture according to the accurate area. Due to the desire for greater precision in picture segmentation, classic image segmentation algorithms, including threshold segmentation, edge segmentation, and clustering segmentation, cannot produce sufficient results. Several machine learning clustering theories, including k-means clustering [6], Markov random fields [7], and Support Vector Machines [8], are encouraged for improving picture segmentation outcomes. In order to obtain better segmentation results from machine learning algorithms, it is often required to manually choose the ROI in order to reduce the majority of interference information in certain complicated images. By substituting artificial ROI selection with object detection, ROIs can be selected automatically. In recent years, object detection has experienced significant breakthroughs because to deep learning. In addition, the Mask R-CNN [9] model detects objects and segments images.

2. Literature Review:

After completing some simple survey in heart diseases prediction in most important for everyone. In this paper what I found, where is the gap, then I will start processing from there to prepare the comparison table which is used to

show various algorithms to approach in machine learning models, with various parameter to resolve the cardiovascular issues to identification with getting some accuracy level. There is little research for the classification and segmentation of the cardiovascular disease dataset. Many of them are model are working good even something to modify and add the parameter then accuracy level is changed, so our work is so good for it even I have to improve and added the necessary parameters to update and change it will give good accuracy and predict the earlier stage.

Younes et al proposed a hybrid method in which two machine learning algorithms support Swarm Optimization and Ant Colony Optimization are effectually combined with the wrapper approach. They are using the UCI machine learning dataset repository. The various data are mixed with the Cleveland clinic foundation for the experiment. After applying the ML model, the classification accuracy was 89.65% in the result of heart diseases.

Jun et al diagnosed heart diseases using the RCNN mask mode algorithm theorem is used in the Ultrasonic image. Therefore R-CNN is a powerful principle in the machine learning model to found ROI, using this RCNN algorithm provides the classification and segmentation of 95.5% of segmentation with ROI wight edge bounders.

JanDorazil et al. proposed a localization algorithm to use form predicting in the ultrasound image in b mode approach to detect the heart artery wall to determine and unknow the about the region and wall tracking method in the ROI. The proposed approach presents the various way to achieve the favourite result optimization with a different machine learning algorithm.

Deepak Mishra et al diagnosed heart diseases segmentation using Deep learning various approaches with 132 ultrasonic images with CNN model. However, they used the vessel segmentation liver image for her implementation in that network result 99.14% -pixel accuracy with a mean accuracy value of 79.16% and IOU value is 69.62% was achieved according to the model.

In order to assess the robustness of the proposed model, Hailong Shang et al introduced the Multi objective mathematical programming (MOMP) model for predicting cardiac medical picture segmentation, which included a synthetic image space of the object with varying concavities and Gaussian noise. Fatma et al in this article used a hybrid approach that involves combining different techniques in the exploiter that fast diagnosis and predicted the heart diseases in this paper will say the classifier different result in the mode with using the various software like Weka and keel.

Table 1: Comparison of study various characteristics, model/algorithm, and the result.

Title / Authors	Type of the Image/Data set/No of Image samples	Feature selection	Algorithm/ Model /Architecture	Accuracy
YounessKhourdifi	CVS file /UCI dataset	FCBF -Fast Correlation - Based feature selection.	PSO/ACO feature selection and classification	Classification 99.65%
Jun Liu,PengFei Li	Ultrasound follicle image	ROI selection	Segmentation/Mask CNN	Segmentation with ROI Accuracy 95.5%
Jan Dorazil, Kamil Riha, Malay k. Dutta	145 Ultrasonic Image	ROI Rectangle[132x132px]	Localization using B mode	Reducing the Error rate to 1.38% of the 15 images and
Deepak Mishra, Sidharth Manohar and Arivnder	Liver US image with 132 images.	A pipelined network comprising with CNN	Segmentation /CNN	Mean 79.16% of accuracy with 69.62 ROI in 132 images.
HailongShang,shiwei Zhao, Hongdi	Tomography and MRI image	Concavities and Gaussian Noise removal	PSO-Particle swarm optimization	Using MOMP model index 0.93% & 0.97% for jaccard's and dice's.
Fatma, Menaouer& Nadda Matta	CVS file /UCI dataset, Cleveland Dataset database	LR, Ada Boosting, Fuzzy classifiers, and ML with PCP and Wra	Hybrid Machine learning technologies	Training Accuracy rate 83.44% with error rate 0.17 testing 78.93% with 0.21.
Xing huang,haozhizhu and jiexin wang	231 tomographic images, 288*288*85 layers, ultrasound image	Greedy algorithm,	VGVF snake model	AOR and MCD values are 97.4% and 3.2 respectively.
Qi Zhenya&Zuoru Zhang	CSV file with different data set as Statlog, Cleveland, Hungarian data set	Ten-fold cross-validation.	Cost-sensitive ensemble method, RF, Logistic regression, SVM, KNN(Hybrid)	Compared with three datasets. Recall and specificity values are compared.
Jiang Hua,TonglinHao,Liangcai Zeng and Guiyu	Dataset using for COCO2017	Semantic Segmentation Algorithm and Neural network.	Fusion network with Yolo Mask model, U-Net, Fast RCNN	-

Xing Huang et al suggested using the model as snake traditional as greedy algorithm as proposed as VGVF snake (vortical gradient vector flow). The implementation they are using 231 tomography images with 288*288*87 layer is used and got the final evaluation of the cardio cavity is segmented as AOR and MCD as 97.4% and 3.2 respectively.

3.Implementation:

At present Machine learning implemented most of the models are developed for classification and segmentation purposes even it will not satisfy the aim in the health care department.

so various versions ML model will be used for object detection in medical diagnosis's some of the stands are provided that using and detecting is necessary to use in the medical field.

Initial phase of the proposed design is Using an AWM filter, the input image is pre-processed and passed to the module. There are two phases involved: noise detection and noise removal. Both phases are integrated into one another. Impulse noise detection yields a binary image with 0 for non-noisy pixel regions and 1 for noisy pixel regions. Using 3 x 3 and 5 x 5 windows, the number of noisy pixels is counted

across all detected pixels, and then an adaptive weighted median filter (AWMs) with a given window size is applied adaptively based on the number of noisy pixels in a region. Impulse noise detection is utilised not only to count the number of noisy pixels, but also to provide a weight of zero to discovered noisy places in 3×3 , 5×5 , and 7×7 windows. Proposed thresholds are based on the absence of noisy pixels in the ranges 1-3, 4-12, and 13 and higher.

AWMF: Steps for AWMF's initial phase are as follows:

- 1) Move a 3×3 window over each pixel $x(m, n)$ at the given location (m, n) .
- 2) Filter the pixels in ascending order for each window $W_3(m, n)$ to obtain $R(m, n)=[r_1(m, n), r_2(m, n), \dots, r_9(m, n)]$.
- 3) Pixel $x(m, n)$ is a noisy candidate if $x(m, n) = r_1(m, n)$ or $x(m, n) = r_9(m, n)$; otherwise, it is a noise-free pixel.

For second stage, it is based on final selection of noisy pixels by processing noise candidates using steps given below

- 1) Move the 11×11 window $W_{11}(m_1, n_1)$ over all noisy candidates at places (m_1, n_1) , and sort the window to get (A)

$$R(m_1, n_1) = [r_1(m_1, n_1), r_2(m_1, n_1), \dots, r_{121}(m_1, n_1)] \quad (A)$$

- 2) The distance vector $D(m_1, n_1)=[d_1(m_1, n_1), d_2(m_1, n_1), \dots, d_{120}(m_1, n_1)]$ where $d_i(m_1, n_1)=r(i+1)(m_1, n_1)-r_i(m_1, n_1)$ is computed.
- 3) Find first the four longest distances $d_{max1} = d_i(m_1, n_1)$, $d_{max2} = d_j(m_1, n_1)$, $d_{max3} = d_k(m_1, n_1)$, and $d_{max4} = d_l(m_1, n_1)$ where $d_{max1} > d_{max2} > d_{max3} > d_{max4}$.
- 4) Select $x(m_1, n_1)$ as a noisy pixels if $(x(m_1, n_1) < w_{min} \text{ or } x(m_1, n_1) > w_{max})$, where $w_{min} = r(p+1)$ and $w_{max} = r_t$. $p = \min[i, j, k, l]$ and $t = \max[i, j, k, l]$.

From this paper the proposed model is YoloV4 (You only look once version 4) it's implemented for classification and segmentation with ultrasonic image used to identify issues in the image. So, this model implementation has two stages in that primary stage have started without doing the help of the

preliminary to detect the object. The secondary stage is the preliminary part for this stage to process input layer, backbone, neck there are to process to detection and classified if an object has been identified in here area. For splitting of the process mainly for increasing the speed to make predictions allowing quickly in real-time.

YOLOv4 is dual and fast as EfficientDet, with the same efficiency. In comparison to YOLOv3, the AP and FPS have increased by 10% and 12%, accordingly. The outstanding speed and accuracy of YOLOv4's fully documented publication are valuable contributions to the scientific community.

A. Input Layer:

The input layer is retrieved the image from the data source and trained the image finally test that image for classification and segmentation into the model in the first layer. Cardiovascular ultrasonic image is the main input source for the first layer with the good resolution even in this image have to noise, the value is so high for using the basic filter to apply and classify the image to process the next layer.

B. Backbone and Neck:

The backbone is the deep learning architecture, it is collected of the three-stage it for Bag of freebies (BoF), Bag of specials (BoS), CSPDarknet53. In the Bag of freebies is increased the training cost and changing the training strategy so for the leaving cost is low. Computer vision and data argumentation are widely used for Deep learning models with increased variability and image order to develop the computer vision and data argumentation to improve training model.

By using weighted linear interpolation of two existing images, all backbone models can mix up images and labels for the augmented image. The combination of two images, noise areas, and memory corruption of labels increases robustness to both training and generating adversarial networks. Focal Loss attempts to correct this significant disparity between the foreground and background courses during training. For most classification problems, cross-entropy is utilised as a loss function. With this function, errors that are highly probable will be penalized more severely

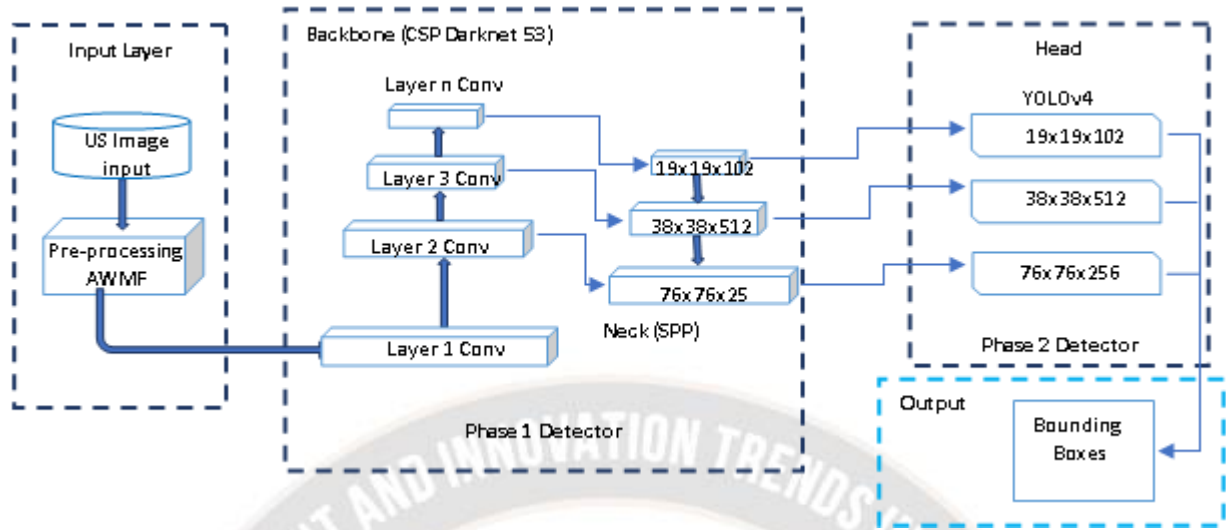


Figure 1: Proposed workflow architecture Diagram

By introducing a $(1-pt)*\gamma$ factor in the Focal loss function, a new cross-entropy is one of the based loss functions is proposed. Based on this coefficient, the correction of misclassified objects is given priority. A focusing parameter γ allows the down-weighting rate for easy examples to be controlled smoothly. When $\gamma = 0$, FL is equal to CE, and as γ increases, the modulating factor's effect also increases. All too often, people think they are right when in fact they are wrong. The model may not learn from the data if it has 100% confidence in its prediction.

YoloV4 model is sort outing problem to Overfitting is a major loss in the calculation in lowers or raises the upper bound to prediction and the lower value is 0.9 and its loss is 0.1 percentage. calculation the real bounding box the position and size difference evaluate the prediction.

It's clear that the IoU loss optimises the bounding box as a whole rather than optimising each of its four coordinates. Consequently, the IoU loss may be able to anticipate the bounding box more accurately than the L2 loss. In addition, when the bounding boxes differ in size, the IoUs are inherently skewed toward $[0, 1]$.

(G) Ground truth: $\tilde{x} = \tilde{x}(\tilde{x}_t, \tilde{x}_b, \tilde{x}_l, \tilde{x}_r)$

(P) Prediction: $x = (x_t, x_b, x_l, x_r)$

$$l_2 \text{ loss} = \| P - G \|_2^2$$

$$IOU \text{ loss} = -\ln\left(\frac{Intersection(P,G)}{Union(P,G)}\right) \quad (1)$$

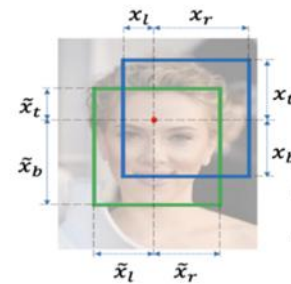


Figure 2: Bound Box Representation for Prediction ground truth region

Mish activation

By design the necessary prerequisites for Dying ReLU and another activation phenomenon are eliminated the hazards and training to make as easier to using MISH's activation function. During the backpropagation phase, neurons that have a large negative bias will not be up-to-date, causing them to be ineffective. Mish has a bound below and an unbounded range above of $[\approx -0.31, \infty]$. Due to a small number of negative information being held on too. Mish characteristics aid in more effective communication and expression. Mish avoids saturation, which slows down training due to essentially no gradients, because it is unbounded above. A strong regularization effect results from being bounded below as well.

As a novel self-regularized non-monotonic activation function, the formula for $f(x) = x \tanh(\text{softplus}(x))$ can be used to define it.

CSPDarknet53 and DenseNet

DenseNet's Cross Stage Partial architecture is built from it by concatenating the prior input with the current one before

moving on to the dense layer. In DenseNet, there are two phases: the dense block and the transition layer, with each dense block consisting of k dense layers. The $(i+1)$ dense layer's input can be obtained by concatenating the output of the i^{th} dense layer with the input of the i^{th} dense layer.

This mechanism can be shown by the equations given below:

$$\begin{aligned} X_1 &= W_1 * X_0 \\ X_2 &= W_2 * [X_0, X_1] \\ \dots & \\ \dots & \\ X_k &= W_k * [X_0, X_1, \dots, X_{k-1}] \end{aligned}$$

Kernel operator $[*]$ indicates a convolution operator, and the values $[x_0-x_n, \dots]$ represent the weights and outputs of a dense layer, with w_i and x_i representing the i^{th} layer's weights and outputs, respectively. We divide the input into two parts x_0' and x_0'' in the CSP, instead of concatenating it with the i^{th} output. A dense layer x_0'' will pass through the first part, and concatenated part x_0' will pass through the second part. The result will be concatenated at the output of the dense layer x_0'' .

Mathematically, this equals the following:

$$\begin{aligned} X_k &= W_k * [X_0'', X_1, \dots, X_{k-1}] \\ X_T &= W_T * [X_0'', X_1, \dots, X_k] \\ X_U &= W_U * [X_0', X_T] \end{aligned}$$

Equation for Partially forwarded in the cross-stage. Consequently, different dense layers will be repeatedly exposed to copies of gradient information.

Neck

Feature maps from different stages of the backbone are gathered in the neck, which is a subset of the bag of specials. In a nutshell, this feature aggregator combines versions of features. In the subsequent sections, we will examine more fully the neck of the object detection pipeline.

Bag of specials

Object detection is improved by using methods from the bag of special methods, which increases computing costs by a small margin but improves accuracy. Obtaining feature maps from various stages is the dominant function of the neck. An average neck is typically made up of a couple of top-down and a couple of bottom-up paths. In a fully interconnected network, it is necessary to have a fixed size image; when detecting objects, it is not necessary to have fixed size images. Due to this issue, we have to scale the images, which may cause a part of the object we are trying to detect to be removed and lead to a less accurate model.

CNN also causes the sliding window to be fixed in size. Our convolution neural networks generate features as part of the output of their computation; these features correspond to the output of our various filters. We could create a filter capable of detecting circular geometric shapes, this filter would produce a feature map highlighting the shapes and keeping the coordinates of the shapes in the image.

SPP - Spatial Pyramid Pooling Layers generate fixed-sized features regardless of the size of our feature maps. Our feature maps will be generated in different representations based on pooling layers such as Max Pooling.

The SPP consists of three levels. Consider the conv5 layer, which contains 256 features. Source from the first step is to pool the feature maps into one value. There are 1, 256 fields in this vector.

- Several feature maps are then pooled to consume four values. The resulting vector is (4, 256).
- The same is true for the pooling of each feature. In this case, the vector has the size (16, 256).
- In step 3, the three vectors are created. This fixed size vector is then concatenated to create the input for the fully connected network.

Head (detector)

In this model can be called an object detector as it finds a region where the object might be but does not tell what kind of object might be present there. Our detection systems are divided into two types: two-stage detectors and one-stage detectors; both types of detectors may be either anchor-based or anchor-free. This section will focus more specifically on the head.

Bag of freebies (BoF)

Those methods that only change the training strategy or raise training costs (but do not affect inference) are considered 'bag of freebies'. Based on the diagram above, there are a plethora of opportunities you can pursue, but we will discuss only the most important ones. During one-stage detection, the head executes dense prediction. In dense prediction, the bounding box would be represented by a vector with the center, height, and width of its predicted area, a confidence score and a label.

Loss of CIoUs

Two new concepts are introduced by the CIoU loss, in contrast to the IoU loss. A bounding box center point distance represents the distance between the actual center point and the predicted center point of the bounding box. Second, we consider the aspect ratio of the true and predicted bounding boxes, and we compare them. The quality of a bounding box

can be measured with these 3 indicators. Equation 2: CIoU loss.

$$L_{CIoU} = 1 - IoU + \frac{\rho^2(b, b^{gt})}{c^2} + \alpha v \quad (2)$$

A trade-off parameter is a positive (α) trade-off parameter, while v measures the consistency of aspect ratio, and their central points are expressed by b and b^{gt} , respectively. The Euclidean distance in $\rho(\cdot)$ is the diagonal length of the smallest enclosing box, while $*$ measures the positive trade-off parameter. Equation 3: consistency of aspect ratio with w being the height and w is the width of the bounding box.

$$v = \frac{4}{\pi^2} \left(\arctan \frac{w^{gt}}{h^{gt}} - \arctan \frac{w}{h} \right)^2 \quad (3)$$

Cross Mini Batch Normalization procedure (CmBN)

If the batch size is too small, the batch normalisation process does not take place. In summary, the sample size biases both the mean and standard deviation estimates. If the sample size is too small, the distribution will probably not be completely representative

The new method known as Self-Adversarial Training (SAT) consists of three stages: two stages of forward movement, and one stage of backward movement. During the first stage of neural network processing, the original image is altered rather than the network weights. By doing so, the neural network performs an adversarial assault on itself by modifying the initial image to create the appearance that it does not contain the object that is being sought after. After the second stage, the neural network is trained to recognise an object based on the initial label on this changed image before the noise is added to the image. This occurs after the second stage.

Using a variety of anchors to support a single fundamental truth: Because convolutional networks are unable to directly forecast the boxes that are linked with certain ratios of images, we make use of anchors that partition the image space in accordance with a variety of different methodologies. we create many anchor boxes by convolution the features maps in order to represent objects of various sizes. Using the IOU, we decide whether to assign certain anchor boxes to objects or backgrounds based upon thresholds below the surface.

$$IoU(\text{truth}, \text{anchor}) > IoU \text{ threshold} \quad (4)$$

Random training shapes

Single-stage detectors often have object detectors that learn from images with a fixed shape. Different image sizes can be used to improve generalization. (YOLO Training on Multiple Scales)

Mish activation

In the latest state-of-the-art models of deep learning, attention layers are very common, primarily in language processing. Yolo models are used to enable the recognition of the most significant features created by convolution layers and their removal.

Max Pooling and Average Pooling are two transforms that must be applied to the output feature map of a convolutional layer to create the Spatial Attention Module (SAM). After concatenating and passing each feature in a convoluted layer, a sigmoid function is applied to highlight the locations of the most important features. For the YoloV4, we use a modified version of SAM (shown in figure 4[D1]) that gets rid of the Max Pooling and Avg Pooling layers. Shapes chosen at random: A fixed image shape is used to train many single-stage object detectors. To make the model more general, we can train it with images of different sizes. (YOLO Training on Multiple Scales).

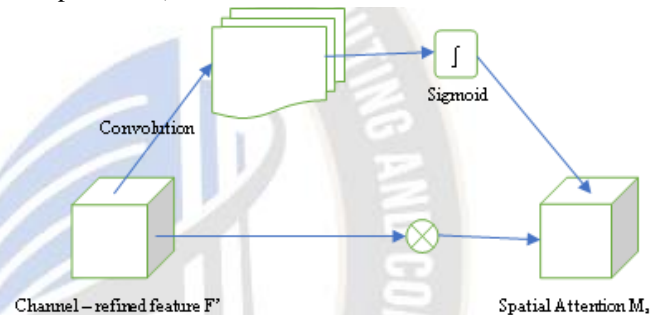


Figure 3: YOLO v4in Modified SAM

DIoU-NMS

Non-Maximum Suppression (NMS) removes overlapping boxes representing the same object, but keeps the box that is most precise compared to the true bounding box.

$$R_{DIoU} = \frac{\rho^2(b, b^{gt})}{c^2} \quad (5)$$

The Equation 4. R_{DIoU} is shown in figure 4 as Assume b and b^{gt} are the central points of B and B^{gt} , where c is the diagonal distance separating the two boxes, and $\rho(\cdot)$ is the Euclidean distance between them.

$$s_i = \begin{cases} s_i, & IoU - R_{DIoU}(M, B_i) < \epsilon, \\ 0, & IoU - R_{DIoU}(M, B_i) \geq \epsilon, \end{cases} \quad (6)$$

From the Equation 5. $DIoU-NMS$ are specifically for test whether the overlap rate minus the distance between the two centers is lower than the threshold ϵ , if so we retain the bounding box otherwise, we delete it.

Performance Evaluation

In this section, the performance of the AWMYolov4 Model and the existing related approaches namely DBN [1] and RCNN model [2] are discussed with three metrics, prediction accuracy, classification Error, Model loss, Precision, Sensitivity and F1 Score. In this paper, Python 3.5 is used as the programming language. For the training, there were a total of 10,000 iterations, and it took 6 hours and 50 minutes. The hardware environment was 8GB RAM and an Intel Core i5 8th generation CPU and NVIDIA GEFORCE GTX GPU.

The table 1 shows the hyperparameters tuned model configuration the AWMF with YOLOv4.

Table 2. Hyperparameters of Yolo4

Parameters	Values
Learning Rate	0.001
Batch size	20
Epochs	100
Optimizer	Adam
Activation Function	Mish
Filter size	3×3, 5×5, 7×7

The prediction frame is usually processed and corrected after more than 250 positive samples and negative samples have been collected. Remove grid sensitivity by replacing *(tx)+cx with *(ty)+cy, and where those numbers are real whole numbers, cx and cy. Consequently, high tx complete values are needed for a parameter bx to approach cx or cx + 1. The solution is to multiply the sigmoid by a factor that is greater than 1.0, thereby eradicating the effect of the grid.

4. Results and Discussion

In this section, the performance of the AWMYolov4 Model and the existing related approaches namely DBN [1] and RCNN model [2] are discussed with some metrics, prediction accuracy, classification Error, False Positive Rate, Precision, Sensitivity, F1 Score and specificity. True positive is TP, False positive is FP, True Negative is TN, and False Negative is FN.

Prediction Time:

Prediction Time is defined as the ratio of number of US images that are correctly identified as diseased image or normal image through segmentation and classification process from given input US images. The prediction accuracy is calculated as,

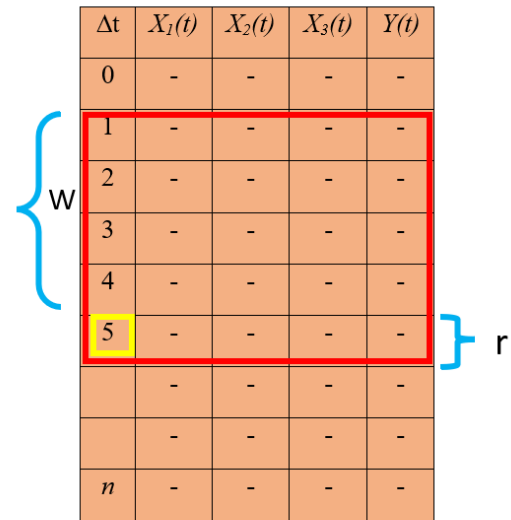


Figure 4: Machine learning approaches for time series

The timestamp at which the prediction will be made will serve as the Window for the value of T that will be predicted (t + window). Our models are fed this information in order to properly represent irregular time series.

$$y(w+r) = f(t_0, \dots, t_w, X_{i,0}, \dots, X_{i,w}, t_{w+r}, Y_{w+r}) \tag{7}$$

$$y(w+r) = f(t_0, \dots, t_w, X_{i,0}, \dots, X_{i,w}, Y_0, \dots, Y_w, t_{w+r}, Y_{w+r}) \tag{8}$$

What our function will do is to flatten all the information contained in the window, which is all the values inside the W window, and the timestamp(s) of when we want to make the prediction.

Table 3. Comparison of Prediction Time

No. of Inputs images	Prediction Time (s)		
	DBN	RCNN	AWMYolov4
100	120.225	130.113	95.30
200	200.350	190.88	170.450
250	256.20	277.503	218.58
350	281.631	300.336	251.205
450	312.55	349.881	298.350

Table 3 lists the experimentally determined prediction times as well as the range of 50–450 US images from the input dataset. The findings of the AWMYoloV4 Model's prediction of time are compared to those of the DBN [1] and RCNN [2] models, two standard approaches. In comparison to current techniques, the suggested AWMYoloV4 Model effectively reduces prediction time. Consider that 100 US images are required for conducting experiments. In comparison to the

standard approaches [1] and [2], which have prediction times of 70% and 80%, respectively, the AWMYoloV4 Model's observed prediction time is 40%. For each technique, varied prediction time results are obtained. Figure 3 shows a graphical representation of forecast time.

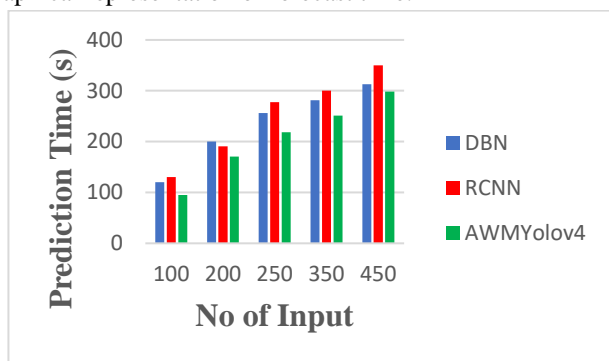


Figure 5: Comparison of Prediction Time

Figure 5 depicts the performance evaluation of prediction time and the number of US photos ranging from 50 to 450. The number of US Images is considered in the horizontal direction, and the prediction time is attained on the vertical axis. The AWMYolov4 Model's prediction time is indicated by the greenish colour column, while the DBN [1] and RCNN [2] models' predictions times are indicated by the blue and red colouring, respectively. When compared to conventional methods, the proposed AWMYolov4 Model has a greater prediction accuracy. This is because the AWMYolov4 Model uses a deep convolutional neural classifier. By removing the noisy pixels, the Adaptive Weighted Mean pre-processing enhances the image quality. The pre-processed image was separated into a number of segments by the YoloV4 backbone module, which uses image segmentation. Following that, the features are retrieved to quickly and accurately do classification for heart disease prediction. Therefore, compared to DBN [1] and RCNN model [2], the suggested AWMYoloV4 Model reduces prediction time by 30% and 15%, respectively.

Classification Error

Table 4. Evaluations of Classification Error

Dataset	Classification Error (%)		
	DBN	RCNN	AWMYolov4
100	9.51	7.21	5.3
200	9.52	7.45	5.1
250	8.76	7.55	4.33
350	8.5	7.1	4.1
450	7.5	7.0	4.0

Table 4 lists the experimentally determined Classification Error using the image ranges between 50–450 US images from the input dataset. The findings of the AWMYoloV4 Model's prediction of time Classification Error are compared to those of the DBN [1] and RCNN [2] models, two standard approaches. In comparison to current techniques, the suggested AWMYoloV4 Model effectively reduces Classification Error. Consider that 100 US images are required for conducting experiments. In comparison to the standard approaches [1] and [2], which have Classification Error of 9.5% and 7.21%, respectively, the AWMYoloV4 Model's observed Classification Error is 5.3%. For each technique, varied Classification Error results are obtained. Figure 4 shows a graphical representation of forecast time.



Figure 6 Classification Error

The number of US Images is considered in the horizontal direction, and the Classification Error is attained on the vertical axis. The AWMYolov4 Model's prediction time is indicated by the greenish colour column, while the DBN [1] and RCNN [2] models Classification Error are indicated by the blue and red colouring, respectively. When compared to conventional methods, the proposed AWMYolov4 Model has a greater Classification Error prediction.

Impact of False positive rate:

False positive rate is computed as the ratio of number of US images that are incorrectly predicted as diseased US image or normal image through performing segmentation and classification process from given input US images. The false positive rate is calculated as,

$$FP_{Rate} = \left(\frac{\text{Number of images incorrectly predicted}}{\text{Number of US Images}} \right) * 100 \quad (9)$$

From (9), 'FP_{Rate}' symbolizes the false positive rate. The false positive rate is measured in terms of percentage (%).

Table 5. Comparison of False Positive rate in percentage

Dataset	False positive rate (%)		
	DBN	RCNN	AWMYolov4
50	71	65	33
100	35	33	21

200	30	27	15
300	24	21	12
500	20	16	10

The achieved results of false positive rate using AWMYolov4 Model are compared to two existing techniques namely the DBN [1] and RCNN model [2]. The proposed AWMYolov4 Model efficiently attains lesser false positive rate than existing methods. Let us consider that number of US images is 200 for experimental consideration. By using AWMYolov4 Model, the observed false positive rate is 30% while the false positive rate of the conventional methods [1] and [2] are 27% and 15% respectively. The different false positive rate results are attained for every method. The graphical illustration of false positive rate is illustrated in figure 7.

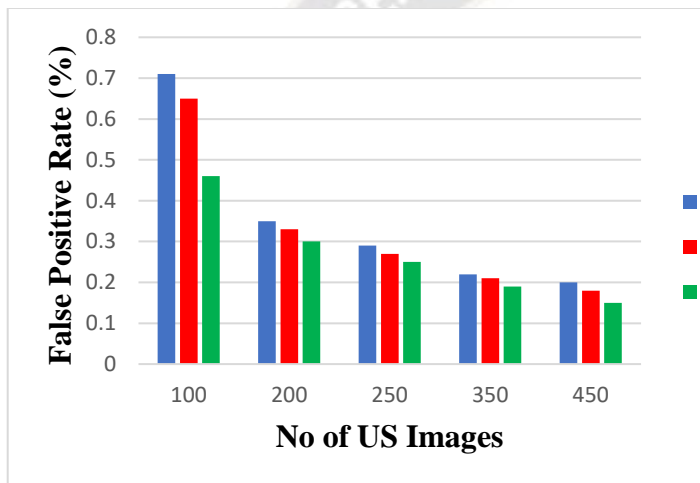


Figure 7. Comparison of Model False Positive Rate(%)

Precision, Sensitivity and F1 Score

After taking into account the classifier's arrangement accuracy and misclassification costs, a final prediction result is generated. For convenience, we set the cost of accurate classification to zero so that we could compare the costs of incorrect categorization for different classifiers. Each classifier has its own section of the MC. When a healthy person is mistakenly labelled as having heart disease, an expensive and pointless course of therapy is initiated. [15] In the second scenario, people with heart disease may be assured they are healthy and thus miss out on the best opportunity for treatment, worsening or possibly causing their condition to die. People who are misclassified face a wide range of prices, thus we set cost1 at 10 and cost2 at 1. The following index is used to evaluate each classifier:

$$E_i = \frac{Accuracy_{i+1} - (MC_i)}{2 \cdot (cost_1 + cost_2)} \quad (10)$$

An independent classifier's overall performance is measured by its mean classification accuracy (MC_i) across the training period, while attitudes toward the effectiveness of the ith classifier are measured by E_i attitudes.

$$MC = \left(\frac{(FP \cdot cost_2 + FN \cdot cost_1)}{(TP + TN + FP + FN)} \right) * 100\% \quad (11)$$

Sensitivity (Recall) or True positive rate

$$Sensitivity (Recall) \text{ or } TPR = \frac{TP}{(TP + FN)} \quad (12)$$

$$Specificity = \frac{TN}{(TN + FP)} \quad (13)$$

$$Accuracy = \frac{(TP + TN)}{(TP + TN + FP + FN)} \quad (14)$$

$$Precision = \frac{TP}{TP + FP} \quad (15)$$

$$F1 \text{ score} = 2 * \frac{Precision * Recall}{Precision + Recall} \quad (16)$$

Table 6. Precision, Recall, F1 Score

Models	Parameters		
	Precision	Sensitivity	F1 Score
DBN	90.03	91.67	90.02
RCNN	91.70	92.54	91.04
AWMYolov4	95.60	94.67	95.15

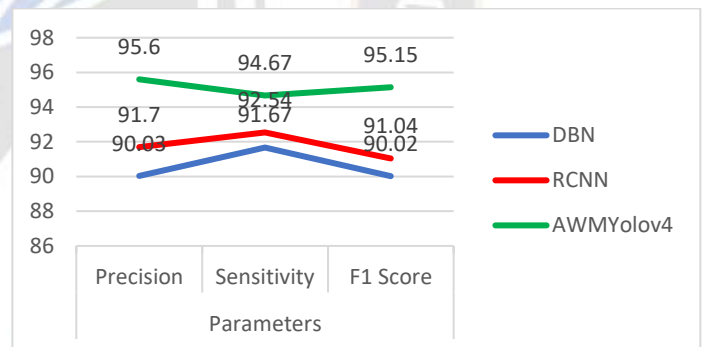


Figure 8. Precision, Sensitivity, F1 Score and specificity

5. Conclusion

This paper uses a machine learning model to predict heart diseases from a US dataset of cardiovascular diseases based on the provided parameters for the patient. It is our goal to classify the ultrasonic image in order to identify the exact defect area within the boundary box and compare the best model with others. The Proposed model compares with different machine learning models showing the best model represented in graph. To evaluate a model, we use the stranded process of selecting features, tuning parameters, and calibrating the model based on the performance of the data. We compare different algorithms in the final stage, with the proposed optimized model by Yolov4 having the highest

accuracy of 96.67%. For the future they add a greater number of data to train the accuracy will increase and error rate will reduce.

List of Abbreviations

AWMF	Adaptive weighted median filter
US	Ultra Sound
CVD	Cardiovascular disease
CNN	Convolutional Neural Network
MRI	Magnetic Resonance Imaging
CPU	Central Processing Unit

Declarations:

Availability of data and materials

Data sharing not applicable to this article as no datasets were generated or analysed during the current study.

Competing interests

The authors declare that they have no competing interests.

Funding

No funding received by any government or private concern.

Author's contribution:

D.D., contributed to the design and implementation of the research, A.K.G. is to analysis of the results and writing of the manuscript.

Acknowledgements

Not applicable.

References

- [1] Liu J., Li P. (2018) A Mask R-CNN Model with Improved Region Proposal Network for Medical Ultrasound Image. In: Huang DS., Jo KH., Zhang XL. (eds) Intelligent Computing Theories and Application. ICIC 2018. Lecture Notes in Computer Science, vol 10955. Springer, Cham. https://doi.org/10.1007/978-3-319-95933-7_4
- [2] Ali A. Samir, Abdullah R. Rashwan, Karam M. Sallam, Ripon K. Chakraborty, Michael J. Ryan and Amr A. Abohany, "Evolutionary algorithm-based convolutional neural network for predicting heart diseases", Computers & Industrial Engineering, Volume 161, November 2021, Pages 1-15
- [3] A. Chanchal, A. S. Singh and K. Anandhan, (2021) "A Modern Comparison of ML Algorithms for Cardiovascular Disease Prediction," 9th International Conference on Reliability, Infocom Technologies and Optimization (Trends and Future Directions) (ICRITO), pp. 1-5, doi: 10.1109/ICRITO51393.2021.9596228.
- [4] Alexander Andreopoulos, John K. Tsotsos,(2008) Efficient and Generalizable Statistical Models of Shape and Appearance for Analysis of Cardiac MRI, Medical Image Analysis, Volume 12, Issue 3, Pages 335-357.
- [5] Aniruddha Dutta, Tamal Batabyal, Meheli Basu and Scott T. Acton, "An efficient convolutional neural network for coronary heart disease prediction", Expert Systems with Applications, Elsevier, Volume 159, November 2020, Pages 1-15
- [6] Anna Karen Gárate-Escamila, Amir Hajjam El Hassani and Emmanuel Andres, "Classification models for heart disease prediction using feature selection and PCA", Informatics in Medicine Unlocked, Elsevier, Volume 19, 2020, Pages 1-14
- [7] Azarmehr, N.(2021) orcid.org/0000-0002-6367-207X, Ye, X., Howard, J.P. et al. "Neural architecture search of echocardiography view classifiers. Journal of Medical Imaging, 8 (3). 034002. ISSN 2329-4302. doi.org/10.1117/1.jmi.8.3.034002.
- [8] C. Wang and Ö. Smedby,(2014) "Model-based left ventricle segmentation in 3D ultrasound using phase image," MICCAI Challenge 10 Computational and Mathematical Methods in Medicine Echocardiogr. Three-Dimensional Ultrasound Segmentation (CETUS), pp. 81-88.
- [9] Carlos Martin-Isla, Victor M. Campello, Cristian Izquierdo, Zahra Raisi-Estabragh, Bettina Baeßler, Steffen E. Petersen, Karim Lekadir. (2020) Image-Based Cardiac Diagnosis With Machine Learning: A Review. Front Cardiovasc Med.; 7: 1. Published online. Jan 24.
- [10] Christyn Akosua Owusu-Agyei, Jin Hou. "Hands Activities Detection in Egocentric Interactions Using YOLOv5", 2021 International Conference on UK-China Emerging Technologies (UCET), 2021
- [11] D. Damodharan and A. Kumar Goel,(2021) "A Novel Approach on classification in Machine Learning model-based USG Cardiogram Images," International Conference on Advance Computing and Innovative Technologies in Engineering (ICACITE), 2021, pp. 947-950, doi: 10.1109/ICACITE51222.2021.9404752.
- [12] Damodharan, D., Goel, A., Kumar, T.(2019) An improved enhancement technique for cardiovascular ultrasonic image analysis based on dcnn International Journal of Advanced Trends in Computer Science and Engineering, 9 (5), pp. 7087-7091.
- [13] Deepika D and Balaji N, "Effective heart disease prediction using novel MLP-EBMDA approach", Biomedical Signal Processing and Control, Elsevier, Volume 72, Part B, February 2022, Pages 1-18
- [14] Dengqing Zhang, Yunyi Chen, Yuxuan Chen, Shengyi Ye, Wenyu Cai, Junxue Jiang, Yechuan Xu, Gongfeng Zheng and Ming Chen, "Heart Disease Prediction Based on the Embedded Feature Selection Method and Deep Neural Network", Journal of Healthcare Engineering,

- Hindawi Publishing Corporation, Volume 2021, 2021, Pages 1-15
- [15] Farman Ali, Shaker El-Sappagh, S. M. Riazul Isla, Daehan Kwak, Amjad Ali, Muhammad Imran and Kyung-Sup Kwak, "A smart healthcare monitoring system for heart disease prediction based on ensemble deep learning and feature fusion", *Information Fusion*, Elsevier, Volume 63, November 2020, Pages 208-222
- [16] Fatma Zahra Abdeldjoud, MenouerBrahmi, Nada Matta.(2020) Chapter 26 A Hybrid Approach for Heart Disease Diagnosis and Prediction Using Machine Learning Techniques, Springer Science and Business Media LLC.
- [17] G. Ramesh, Karanam Madhavi, P. Dileep Kumar Reddy, J. Somasekar, Joseph Tan "Improving the accuracy of heart attack risk prediction based on information gain feature selection technique", *Materials Today: Proceedings*, Elsevier, February 2021, Pages 1-15
- [18] Hailong Shang, Shiwei Zhao, Hongdi Du, Jinggang Zhang, Wei Xing, Hailin Shen. "A new solution model for cardiac medical image segmentation", *Journal of Thoracic Disease*, 2020
- [19] IbomoiyeDomorMienye, Yanxia Sun and Zenghui Wang, "Improved sparse autoencoder based artificial neural network approach for prediction of heart disease", *Informatics in Medicine Unlocked*, Elsevier, Volume 18, 2020, Pages 1-15
- [20] Ivar M. Salte, Andreas Østvik, Erik Smistad, et al (2021) "Artificial Intelligence for Automatic Measurement of Left Ventricular Strain in Echocardiography, *JACC: Cardiovascular Imaging*", Volume 14, Issue 10, Pages 1918-1928, ISSN 1936-878X, <https://doi.org/10.1016/j.jcmg.2021.04.018>.
- [21] J. Dorazil, K. Řiha and M. K. Dutta,(2019) "Common Carotid Artery Wall Localization in B-mode Ultrasound Images for Initialization of Artery Wall Tracking Methods," 2019 42nd International Conference on Telecommunications and Signal Processing (TSP), pp. 605-608, doi: 10.1109/TSP.2019.8769077.
- [22] K. Arul Jothi, S. Subburam, V. Umadevi and K. Hemavathy, "Heart disease prediction system using machine learning", *Materials Today: Proceedings*, Elsevier, February 2021, Pages 1-15
- [23] Karen Garate-Escamilla, A., Hassani, A. H. E., &Andres,(2020) E. Classification models for heart disease prediction using feature selection and PCA. *Informatics in Medicine Unlocked*, 100330. doi: 10.1016/j.imu.2020.100330
- [24] Khourdifi, Youness and Mohamed Bahaj.(2019) "Heart Disease Prediction and Classification Using Machine Learning Algorithms Optimized by Particle Swarm Optimization and Ant Colony Optimization." *International Journal of Intelligent Engineering and Systems*: n. pag.
- [25] Litjens G, Ciompi F, Wolterink JM, et al.(2019) State-of-the-art deep learning in cardiovascular image analysis. *JACC Cardiovasc Imaging*. 2019;12(8 Pt 1):1549–65.
- [26] Madani, A., Arnaout, R., Mofrad, M. et al. (2018) "Fast and accurate view classification of echocardiograms using deep learning". *npj Digital Med* 1, 6. <https://doi.org/10.1038/s41746-017-0013-1>.
- [27] Na Liu, Jiang Shen, Man Xu, Dan Gan, Er-Shi Qi, Bo Gao.(2018) Improved Cost-Sensitive Support Vector Machine Classifier for Breast Cancer Diagnosis, *Mathematical Problems in Engineering*.
- [28] NabaouiaLouridi, Samira Douzi and Bouabid El Ouahidi, "Machine learning-based identification of patients with a cardiovascular defect", *Journal of Big Data*, Springer, Volume 8, Issue 133, 2021, Pages 1-12
- [29] Partho P. Sengupta, Y. Chandrashekar,(2022) "Imaging With Deep Learning: Sharpening the Cutting Edge, *JACC: Cardiovascular Imaging*,"15, Issue 3,,547-549, ISSN 1936-878X, doi.org/10.1016/j.jcmg.2022.02.001.
- [30] Qi Zhenya, Zuoru Zhang. (2021) A hybrid cost-sensitive ensemble for heart disease prediction, *BMC Medical Informatics and Decision Making*. doi.org/10.1186/s12911-021-01436-7
- [31] R. Indrakumari, T. Poongodi and Soumya Ranjan Jena,(2020) "Heart Disease Prediction using Exploratory Data Analysis", *Procedia Computer Science*, Elsevier, Volume 173, Pages 130-139
- [32] Renji P. Cherian, Noby Thomas and Sunder Venkitachalam, "Weight optimized neural network for heart disease prediction using hybrid lion plus particle swarm algorithm", *Journal of Biomedical Informatics*, Elsevier, Volume 110, October 2020, Pages 1-15
- [33] RiteshSonawane and Hitendra Patil., "Automated heart disease prediction model by hybrid heuristic-based feature optimization and enhanced clustering", *Biomedical Signal Processing and Control*, Elsevier, Volume 72, Part A, February 2022, Pages 1-15
- [34] SaiyedFaiayazWaris and S. Koteeswaran, "Heart disease early prediction using a novel machine learning method called improved K-means neighbor classifier in python", *Materials Today: Proceedings*, Elsevier, March 2021, Pages 1-15
- [35] Samuel Lalmuanawma, Jamal Hussain, LalrinfelaChhakchhuak.(2021) Applications of Machine Learning and Artificial Intelligence for Covid-19 (SARS-CoV-2) pandemic: A review, *Chaos, Solitons & Fractals*.
- [36] Siboprasad Patro, Gouri Sankar Nayak and NeelamadhabPadhy, "Heart disease prediction by using novel optimization algorithm: A supervised learning prospective", *Informatics in Medicine Unlocked*, Elsevier, Volume 26, 2021, Pages 1-12
- [37] Slomka PJ, Miller RJ, Isgum I, Dey D.(2020) Application and Translation of Artificial Intelligence to Cardiovascular Imaging in Nuclear Medicine and Noncontrast CT. *Semin Nucl Med*. 2020 Jul;50(4):357-366. doi: 10.1053/j.semnucmed.2020.03.004.
- [38] Talha Karadeniz, Gul Tokdemir and HadiHakanMaras,(2021) "Ensemble Methods for Heart Disease Prediction", *New Generation Computing*, Springer, Volume 39, Pages 569–581

- [39] VirenViraj Shankar, Varun Kumar, Umesh Devagade, Vinay Karanth and K. Rohitaksha(2020) "Heart Disease Prediction using CNN Algorithm", SN Computer Science, Springer, Volume 1, Issue 170, Pages 1-15.
- [40] godala, sravanthi, & Vaddella, R. P. V. (2022). A Study on Intrusion Detection System in Wireless Sensor Networks. *International Journal of Communication Networks and Information Security (IJCNIS)*, 12(1).
- [41] Wenqi Li, Ming Zuo, Hongjin Zhao, Qi Xu and Dehua Chen, "Prediction of coronary heart disease based on combined reinforcement multitask progressive time-series networks", *Methods*, Elsevier, Volume 198, February 2022, Pages 96-106
- [42] Mishra, A., Singh, A., & Ujlayan, A. (2021). A Pragmatic Approach for EEG-based Affect Classification. *International Journal of Intelligent Systems and Applications in Engineering*, 9(4), 165–170. <https://doi.org/10.18201/ijisae.2021473635>
- [43] Xiao-Yan Gao, Abdelmegeid Amin Ali, Hassan Shaban Hassan, and Eman M. Anwar, "Improving the Accuracy for Analyzing Heart Diseases Prediction Based on the Ensemble Method", *Complexity*, Hindawi Publishing Corporation, Volume 2021, 2021, Pages 1-16
- [44] Xing Huang, Haozhi Zhu, Jiexin Wang. "Adoption of Snake Variable Model-Based Method in Segmentation and Quantitative Calculation of Cardiac Ultrasound Medical Images", *Journal of Healthcare Engineering*, 2021
- [45] M. J. Traum, J. Fiorentine. (2021). Rapid Evaluation On-Line Assessment of Student Learning Gains for Just-In-Time Course Modification. *Journal of Online Engineering Education*, 12(1), 06–13. Retrieved from <http://onlineengineeringeducation.com/index.php/joe/article/view/45>
- [46] Yar Muhammad, Muhammad Tahir, Maqsood Hayat and KilTo Chong, "Early and accurate detection and diagnosis of heart disease using intelligent computational model", *Scientific Reports*, Springer, Volume 10, Issue 19747, 2020, Pages 1-15
- [47] Ye Z, Kumar Y, Sing G, et al.(2020) Deep echocardiography: a first step toward automatic cardiac disease diagnosis using machine learning. *J Internet Technol*. 21(6):1589–600.
- [48] Zhou, J., Du, M., Chang, S. et al.(2021) "Artificial intelligence in echocardiography: detection, functional evaluation, and disease diagnosis. *Cardiovasc Ultrasound*". 19, 29. <https://doi.org/10.1186/s12947-021-00261-2>.
- [49] Zhuang Z, Jin P, Joseph Raj AN, Yuan Y, Zhuang S.(2021) Automatic Segmentation of Left Ventricle in Echocardiography Based on YOLOv3 Model to Achieve Constraint and Positioning. *Comput Math Methods Med*. doi: 10.1155/2021/3772129. PMID: 34055033; PMCID: PMC8143884.